A novel adaptive dual extended Kalman filtering algorithm for the Li-ion battery state of charge and state of health co-estimation.

XU, W., WANG, S., JIANG, C., FERNANDEZ, C., YU, C., FAN, Y. and CAO, W.

2021

A novel adaptive dual extended Kalman filtering algorithm for the Li-ion battery state of charge and state of health co-estimation

Wenhua Xu, Shunli Wang, Cong Jiang, Carlos Fernandez, Chunmei Yu, Yongcun Fan, Wen Cao

Summary

Accurate prediction of the state of health (SOH) of Li-ion battery has an important role in the estimation of battery state of charge (SOC), which can not only improve the efficiency of battery usage but also ensure its safety performance. The battery capacity will decrease with the increase of charge and discharge times, while the internal resistance will become larger, which will affect battery management. The capacity attenuation characteristics of Li-ion batteries are analyzed by aging experiment. Based on the equivalent circuit model and online parameter identification, a novel adaptive dual extended Kalman filter algorithm is proposed to consider the influence of the battery SOH on the estimation of the battery SOC, and the SOC and SOH of the Li-ion battery are estimated collaboratively. The feasibility and accuracy of the model and algorithm are verified by experiments. The results show that the algorithm has good convergence and tracking. The maximum error in the estimation of the SOC is 2.03%, and the maximum error of the Ohmic resistance is 15.3%. It can better evaluate the SOH and SOC of Li-ion battery and reduce the dependence on experimental data, providing a reference for the efficient management of Li-ion batteries.

1 INTRODUCTION

The development of green energy and the protection of the environment occupy an important place in the world development plan. The search for new sources of energy to replace high-emitting fuels is a major concern for all countries. Li-ion batteries have received a lot of attention and application in new energy field because of its high energy density, long life, high-output power, and high-cost-performance, and has great development prospect. With the widespread application of Li-ion batteries in various industries, the detection of their health condition has been paid more and more attention.[1] Researchers have conducted in-depth studies on battery management, such as Zhang et al.[2] studied battery heating for lithium-ion batteries based on multistage alternative currents, and Shen et al.[3] studied battery aging assessment for real-world electric busses based on incremental capacity analysis (ICA) and radial basis function neural network. Among them, it is of great significance to accurately estimate the state of charge (SOC) and state of health (SOH) of Li-ion batteries in giving full play to the performance of batteries and achieving efficient utilization and safe management of Li-ion batteries.

As Li-ion batteries often operate under complex power conditions, their state detection is easily affected by environmental noise.[4] In addition, the internal electrochemical reaction of the Li-ion battery is complicated, often accompanied by polarization effects and ohmic effects, combined with variable discharge currents under complex conditions, internal battery temperature, self-discharge of the battery, and repeated use of materials to cause aging.[5, 6] Due to the interference of other factors, accurate real-time estimation of the SOC and SOH of Li-ion batteries is facing greater difficulties.[7, 8] However, due to the complex internal

structure of the Li-ion battery, it often exhibits strong nonlinear characteristics when used under complicated conditions, making it difficult for the traditional equivalent model to fully and correctly characterize the characteristics of the Li-ion battery. There are still many problems and deficiencies in equivalent modeling and state estimation. Researchers have done a lot of research on this.[9-12] Therefore, how to establish an equivalent model for the performance characteristics of Li-ion batteries and estimate the battery state with the correct and appropriate algorithm, real-time monitoring and safety control of Li-ion batteries, and improve the efficiency of the battery is of great significance.

As early as the beginning of the 20th century, the global Li-ion battery industry has reached $15.3 billion. Its application range has penetrated into various industries, such as new energy vehicles, aviation, and household appliances. In the process of Li-ion battery state estimation, battery equivalent modeling plays an important role. The accurate estimation of the SOC depends to a large extent on the degree to which the equivalent model characterizes the dynamics of the battery,[13] and the accurate estimation of SOH depends on the accurate estimation of SOC. Common battery models in current applications include electrochemical models,[14, 15] neural network models, and equivalent circuit models.[16-18] Zhang et al.[19] used the theory of electrochemical impedance spectroscopy to guide and improve the equivalent circuit model. Kim et al.[20] studied an enhanced hybrid battery model. The equivalent circuit model shows the complex dynamic characteristics of the battery during use, specifically the dynamic response in the circuit loop. Based on the established equivalent circuit, the state space equations of the circuit are obtained by applying the knowledge of circuit science to study the battery characteristics.

The commonly used methods in the estimation of Li-ion battery SOC are open-circuit voltage method, Ampere-hour (Ah) integral method,[21] equivalent model-based methods, and data-driven methods. The equivalent model-based methods are mainly Kalman filter (KF) method, extended Kalman filter (EKF) method.[22-25] The data-driven methods mainly include the artificial neural network method.[26] Sun et al.[27] proposed an intelligent adaptive extended KF method that can detect the moment of distribution change of EIS by the maximum likelihood function. Li et al.[28] proposed two recursive neural network with gated recursive units combined with the Coulomb counting method to estimate SOC. Ayob et al.[29] used two popular neural network algorithms to estimate the SOC. The open-circuit voltage method uses the functional relationship between the open-circuit voltage and the SOC to obtain the SOC value by obtaining the open-circuit voltage value of the battery to achieve the purpose of estimation.[30, 31] The Ah integration method starts from the definition and calculates the SOC by integrating the current in time, which is a more traditional method. The KF method obtains the optimal solution in the sense of minimum variance through continuous iterative operations.[32] Due to the complex electrochemical reaction inside the battery, it often exhibits strong nonlinear characteristics. Coupled with some defects of the traditional algorithms, the above methods often cannot accurately estimate the SOC of Li-ion batteries when dealing with nonlinear systems. Therefore, in recent years, researchers have proposed some improved algorithms on the basis of the above algorithms for the problem of accurate estimation of the SOC of Li-ion batteries.[33-39]

The current methods for estimating battery SOH mainly include empirical model-based methods,[40] equivalent circuit model-based methods, data-driven estimation methods[41] and ICA method.[42] The empirical model obtains the change of battery performance state through the analysis of large experimental data, and summarizes the change law of the battery SOH. It has the advantages of low-modeling difficulty and wide application range, but the physical meaning of the empirical model is not clear, relying on experimental data, and lacks precision and accuracy in evaluating the results. The method based on the equivalent circuit model

simulates the relationship between the external parameters of the battery and the internal state quantity through the circuit. On the basis of the equivalent circuit model, the filter is used to realize the SOH estimation. The filter algorithms mainly include KF,[43, 44] Particle filter (PF), and least square (LS).[45] Data-driven methods include autoregressive models, artificial neural networks,[46] support vector machines (SVMs)[47] and Gaussian process regression.[48, 49] Tan et al[50] establish a support vector regression algorithm for online SOH estimation. Richardson et al[51] proposed a gaussian process regression for in situ capacity estimation, which uses voltage measurement to estimate battery capacity in a short period of time during the constant current operation. These methods have received more and more attention because they do not involve complex physical models. However, the effectiveness of these methods largely depends on the quality and quantity of the test data, and the derived models usually require a lot of computational intensity. In order to avoid dependence on data, an iterative algorithm based on the equivalent circuit model is selected to estimate the battery SOH. Since the state estimation relies heavily on the equivalent model, the model selection and construction are important.[52] Therefore, the equivalent circuit modeling and state estimation of batteries under various complex operating conditions need to be further developed.

The equivalent circuit models include the internal resistance model, Thevenin model, and PNGV model[53]. The internal resistance model only takes into account the simple operating characteristics of the battery and the structure is relatively simple. On this basis, the Thevenin model simulates the dynamic characteristics of the battery to a certain extent by introducing resistance and capacitance (RC) parallel circuit to describe the polarization effect within the battery. Compared with the complex structure of the PNGV model, the Thevenin model is a nonlinear low-order model with lower computational complexity and the required accuracy. Based on the consideration of computational complexity and characterization effect, the Thevenin equivalent circuit model is established to characterize the dynamic characteristics of the battery. The results show that the characterization effect is good.

Aiming at the goal of accurately describing the SOH and the SOC of ternary Li-ion battery, joint estimation is considered, and the adaptive dual extended Kalman filter (ADEKF) algorithm is used to collaboratively estimate the SOC and the SOH of Li-ion battery, and to estimate both states simultaneously and improve the accuracy of the estimation results. This algorithm avoids dependence on experimental data and reduces computational complexity in practical applications.

2 MATHEMATICAL ANALYSIS

2.1 Equivalent circuit modeling

The accurate estimation of SOC depends largely on the representation of the dynamic characteristics of the battery by the equivalent model. The Thevenin model consists of a Rint model connected to parallel with a RC loop. The basic idea is to use an RC parallel circuit to characterize the polarization effect of the battery during use, which to makes up for the shortcomings of the Rint model that cannot characterize the dynamic characteristics of Li-ion battery as shown in Figure 1.

In Figure 1, U_{oc} represents the open-circuit voltage, U_L represents the terminal voltage, R_o is the ohmic internal resistance, and U_R is the ohmic voltage. The RC parallel circuit consists of a polarization resistor R_1 and a polarization capacitor C_1 to characterize the polarization effect of the Li-ion battery, wherein U_1 is a polarization voltage.

The expressions for the voltage and current of the equivalent circuit are obtained as shown in Equation (1) by analyzing the Thevenin equivalent circuit model through Kirchhoff law.

(1)where the open-circuit voltage is a nonlinear function of SOC, and the open-circuit voltage can be calculated from the SOC value.

2.2 Online parameter identification

In order to better observe the prediction of internal resistance, the online parameter identification method is used to identify the battery model parameters. The identification method is the recursive least square (RLS) method. First, according to the equivalent circuit model in Figure 1, the output equation of the circuit is shown in Equation (2).

(2)The direction of the current in Equation (2) is opposite to that in Figure 1. Substituting $s = 2(1-z^{-1})/T(1+z^{-1})$ into the above equation, Equation (3) can be obtained.

(3)In the formula, $E(s) = U_L(s)-U_{oc}(s)$. According to the principle of RLSs, let:

(4)Combining Equation (3) and (4), we can get the equation that needs to be identified as shown in Equation (5).

(5)The RLSs method can be used to estimate the values of θ_1, θ_2, and θ_3, and then according to Equation (3), the parameters in the circuit can be calculated as shown in Equation (6).

(6)

2.3 Adaptive dual extended KF

When the battery capacity is less than 80%, the battery is considered to be completely aged. The SOH can be defined by increasing internal resistance, which is calculated as shown in Equation (7).

(7)In this equation, R_n is the rated internal resistance of the new battery, R_e is the internal resistance corresponding to the decommissioned state of the battery, and R_o is the present internal resistance of the battery. It is measured that the internal resistance of the battery used is 3.545 mΩ when it is completely aging. The definition of SOC is shown in Equation (8).

(8)The extended KF is an improvement of the KF algorithm. The KF method itself is an estimation method for linear systems. When the estimated system is a nonlinear system, the system needs to be linearized first, and the extended KF method introduces the linearization process of nonlinear systems. The dual extended Kalman is two extended Kalman algorithms used to estimate SOC and SOH, respectively. The schematic diagram of the adaptive dual extended Kalman algorithm is shown in Figure 2

The adaptive extended KF estimates SOC by taking it as state variable and battery internal resistance as algorithm input. The extended KF estimates the battery internal resistance R_o by taking SOC as the input value and battery internal resistance as the state variable, and obtaining the current SOH by predicting the battery internal resistance.

First, the state space equation is established according to the equivalent circuit model, and the state space equation is as shown in Equation (9).

(9)

The first and second equations are respectively the state equations for estimating SOC and SOH, and the third equation is the observation equation of the system. Since the internal resistance of the battery changes slowly, an external noise r is added to the state equation for estimating internal resistance to simulate the change in the internal resistance of the battery, where, w_k, r_k, and v_k are Gaussian white noises with zero mean value.

According to the equation of state, the coefficient matrix can be obtained as shown in Equation (10).

(10)A, B, and C are the coefficient matrices of the state equation and the observation equation, respectively.

The specific estimation process of ADEKF is as follows: First, the state and covariance are initialized as shown in Equation (11).

(11)

The iterative process is divided into the time update process and the measurement update process. The time update process is the prediction of state and covariance, as shown in Equation (12).

(12)The measurement update process includes Kalman gain, state, and covariance update, as shown in Equation (13).

(13)Through continuous update iterations to correct the predicted value, accurate SOC and SOH estimates can be obtained.

3 EXPERIMENTAL ANALYSIS

3.1 Test equipment and platform

The new ternary lithium-ion battery is selected for testing, and the battery has a rated capacity of 45 Ah. The equipment used in the experiment include the power cell large-rate charge and discharge tester, and a three-layer independent temperature control high and low-temperature test chamber (BTT-331C), as shown in Figure 3. As the parameters of the battery are affected by temperature, the experiment is conducted at a constant temperature of 25°C, and parameters change need to be considered at different temperatures.[54, 55]

The battery will age due to cyclic use and other reasons, and the actual discharge capacity of the battery will have a large deviation from deviated from the rated capacity. The true discharge capacity of the battery is important for the estimation of the SOC of the Li-ion battery. Therefore, the capacity calibration experiment of the Li-ion battery should be conducted first. In this research, in order to better observe the change of resistance, the online parameter identification method is adopted.

3.2 Parameter identification

The new Li-ion battery capacity is first tested, and the battery actual discharge capacity is measured as 45 Ah at 25°C. The pulse discharge test is conducted to Li-ion battery, and the experimental flow chart is shown in Figure 4.

The curves of the current and terminal voltage of the pulse discharge test are shown in Figure 5. During the experiment, the direction of the charging current is positive.

In this figure, I represents current and U represents terminal voltage. Obviously, the battery voltage will gradually stabilize after a long period of shelving at the end of discharge, which indicates that its internal chemical reactions and thermal effects have basically reached equilibrium. The battery voltage at this time is its open-circuit voltage, and the relationship between the open-circuit voltage and the SOC can be obtained as shown in Equation (14).

(14)According to the RLS online parameter identification principle, various parameters of the model can be obtained. In order to verify the effectiveness of the constructed Thevenin equivalent circuit model in characterizing the battery in real operating conditions, the voltage and current data under the condition of cyclic discharge are imported into the equivalent battery model constructed in MATLAB/Simulink, and the online parameter identification results and the model are verified.

The model output voltage is compared with the actual terminal voltage values and the errors are analyzed, as shown in Figures 6 and 7.

Figure 6 shows the comparison between the model estimated value and the actual value of the battery terminal voltage under the condition of the cyclic discharge shelving experimental condition. The UL2 line is the simulated value of the voltage output from the constructed model, while UL1 is the real battery terminal voltage. Figure 7 shows the error curve of both. From the figure, it can be seen that the simulated value tracks the actual value well, with an average estimated error of about 0.03 V, which can basically characterize the battery in actual operation. The large initial error is due to the initial value error of the parameters in the online parameter identification, and the error decreases after the parameters converge. Through the analysis of the two voltages' comparison result and the error, it is found that the voltage estimation error will increase after the battery is discharged. Because the battery voltage changes drastically at the end of the discharge, the model estimation value lags behind the effect, leading to larger estimation errors.

3.3 Aging test analysis

The new Li-ion battery is charged and discharged for several months at a rate of 1C under a normal temperature environment until the Li-ion battery has aged to its discharge capacity of 80% of the initial capacity, which is regarded as the end of its life as a Li-ion battery. During the cycle of discharge, the capacity test is performed every 100 times, and the aging characteristic curve as shown in Figure 8 is obtained.

As can be seen from Figure 8, the battery capacity has decayed to 80% of its rated capacity after 460 cycles of charge and discharge, and the battery has completely aged. With the continuous decrease of the capacity, the shorter the time for the battery to reach the charging and discharging cut-off voltage, the battery capacity will further decrease.

3.4 Complex condition experiment

In order to verify the estimation effect of the algorithm, experimental analysis is conducted with the Beijing Bus Dynamic Stress Test (BBDST) condition.

The BBDST condition is obtained by processing the data collected from the starting, acceleration, sliding, braking, rapid acceleration, and stopping of the Beijing bus. According to the actual situation, the power of each step is reduced to simulate the BBDST condition. The specific working steps are shown in Table 1.

TABLE 1. BBDST condition

P_b/kW	P_c/W	t/s	T/s	Status
37.5	37.5	21	21	Starting
72.5	72.5	12	33	Acceleration
4.5	4.5	16	49	Sliding
−15	−15	6	55	Braking
37.5	37.5	21	76	Acceleration
4.5	4.5	16	92	Sliding
−15	−15	6	98	Braking

72.5	72.5	9	107	Acceleration
92.5	92.5	6	113	Rapid acceleration
37.5	37.5	21	134	Acceleration
4.5	4.5	16	150	Sliding
−15	-15	6	156	Braking
72.5	72.5	9	165	Acceleration
92.5	92.5	6	171	Rapid acceleration
37.5	37.5	21	192	Acceleration
4.5	4.5	16	208	Sliding
−35	−35	9	217	Braking
−15	−15	6	229	Braking
4.5	4.5	71	300	Stopping

In Table 1, P_b is the battery output power under the real bus starting, acceleration, and skidding conditions. P_c is the actual power of the experiment on the Li-ion battery, t represents the duration of each condition, and T represents the cumulative duration. The experimental data of BBDST are shown in Figures 9 and 10.

The BBDST condition data are substituted into the algorithm to obtain the estimation results. The estimation of SOC is shown in Figure 11.

In Figure 11, S1 is the SOC estimated by the ADEKF algorithm, and S2 is the SOC estimated by dual extended KF algorithm, and S3 is the true SOC. Err1 is the error of the ADEKF algorithm to estimate SOC, and Err2 is the error of dual extended KF algorithm. Under the BBDST condition, ADEKF tracks the SOC of the battery better than the dual extended KF algorithm, and the estimation error is within 0.0203, so it can track the SOC of the battery well under this condition.

In Figure 12, R_o1 is the estimated internal resistance by the ADEKF algorithm, and R_o2 is the estimated internal resistance by the dual extended KF algorithm, and R_o3 is the measuring internal resistance. Err1 is the error of the ADEKF algorithm to estimate the internal resistance and Err2 is the error of the dual extended KF algorithm. It can be seen that ADEKF has good convergence in estimating internal resistance, and the internal resistance can be estimated. After convergence, the error is kept within 15.3%. Compared with the dual extended KF algorithm, ADEKF can better estimate the internal resistance without major fluctuations. However, SOH can be estimated by calculating the estimated value of ohmic resistance as shown in Figure 13.

In Figure 13, SOH1 is the real SOH and SOH2 is the SOH estimated by the ADEKF algorithm. To sum up, compared with the ADEKF algorithm, this algorithm has a smaller error and no divergence occurs at the end of the estimation.

4 CONCLUSIONS

The accurate estimation of SOC and SOH provides an important guarantee for the safety management of Li-ion. The aging characteristics of Li-ion batteries are analyzed. Based on Thevenin equivalent circuit model and online parameter identification method, an ADEKF is proposed that estimates SOC and SOH simultaneously. The results show that the algorithm can simultaneously estimate the SOC and SOH. The error of estimating SOC is within 2.03%, and the error of estimating the SOH characterization parameter ohmic internal resistance is within 15.3%. The algorithm has good convergence and can give a good reference to the battery management system, avoiding the reliance on experimental data and reducing the computational complexity in practical application. It is more effective to ensure the safety of battery use and provide a basis for the estimation of remaining useful life.

ACKNOWLEDGEMENTS

The work was supported by National Natural Science Foundation of China (No. 61801407), China Scholarship Council (No. 201908515099), Fund of Robot Technology Used for Special Environment Key Laboratory of Sichuan Province (No. 18kftk03), and Natural Science Foundation of Southwest University of Science and Technology (No.17zx7110, 18zx7145).

Figures

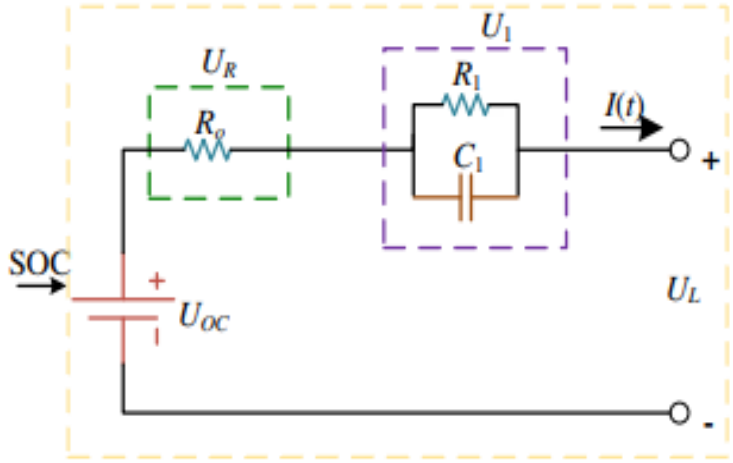

FIGURE 1 Equivalent circuit model. SOC, state of charge
[Colour figure can be viewed at wileyonlinelibrary.com]

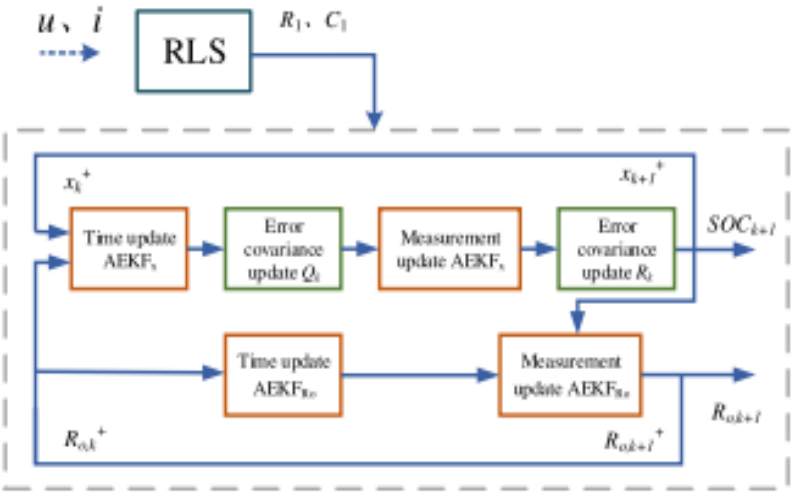

FIGURE 2 Flow chart of ADEKF algorithm. ADEKF, adaptive dual extended Kalman filter [Colour figure can be viewed at wileyonlinelibrary.com]

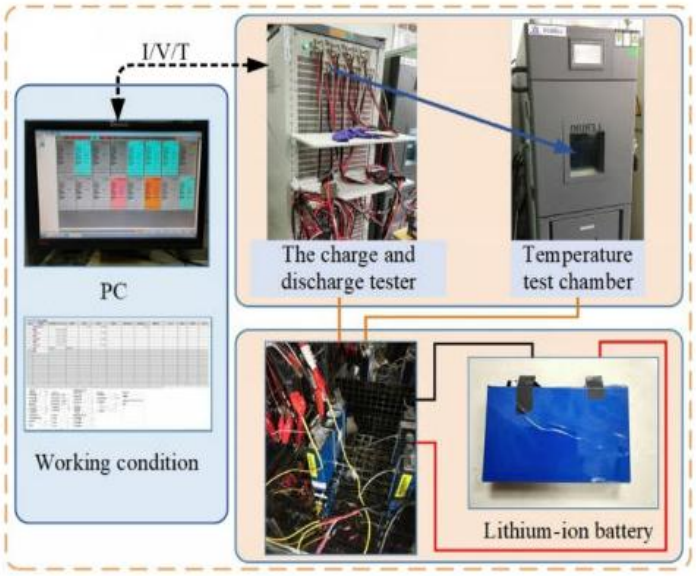

FIGURE 3 Experimental equipment [Colour figure can be viewed at wileyonlinelibrary.com]

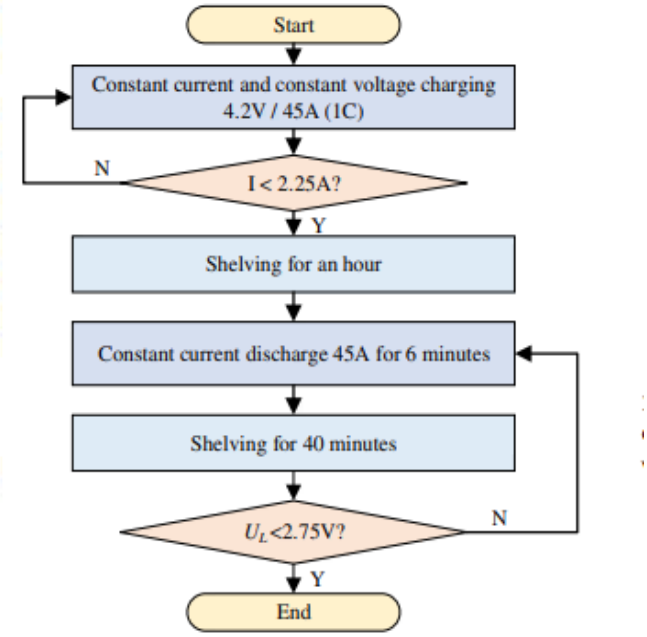

FIGURE 4 Flow chart of pulse discharge test [Colour figure can be viewed at wileyonlinelibrary.com]

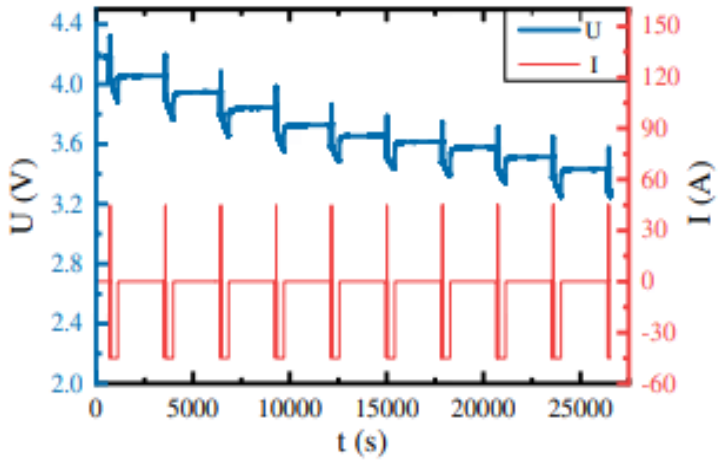

FIGURE 5 Current and terminal voltage curves of pulse discharge test [Colour figure can be viewed at wileyonlinelibrary.com]

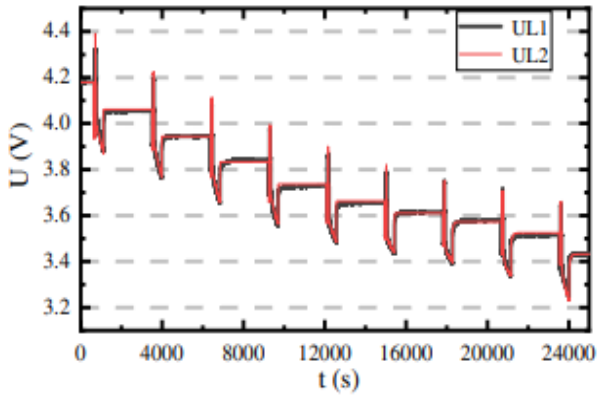

FIGURE 6 Comparison of model voltage effect [Colour figure can be viewed at wileyonlinelibrary.com]

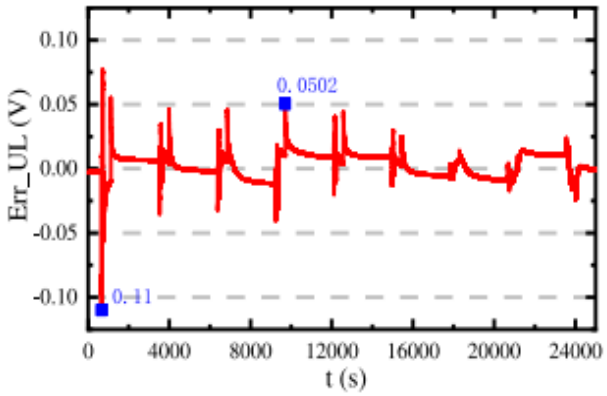

FIGURE 7 Voltage error [Colour figure can be viewed at wileyonlinelibrary.com]

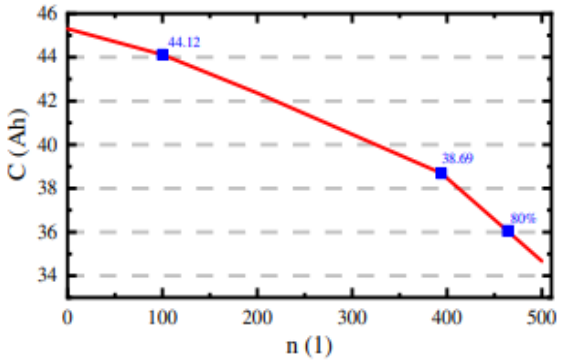

FIGURE 8 The aging characteristic curve [Colour figure can be viewed at wileyonlinelibrary.com]

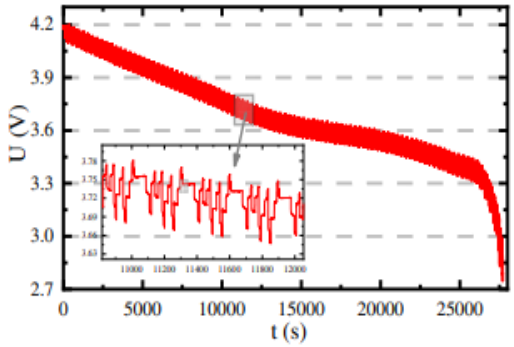

FIGURE 9 The current curve of BBDST condition. BBDST, Beijing Bus Dynamic Stress Test [Colour figure can be viewed at wileyonlinelibrary.com]

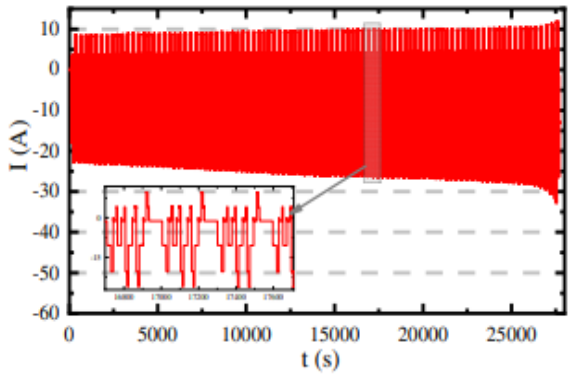

FIGURE 10 Voltage curve of BBDST condition. BBDST, Beijing Bus Dynamic Stress Test [Colour figure can be viewed at wileyonlinelibrary.com]

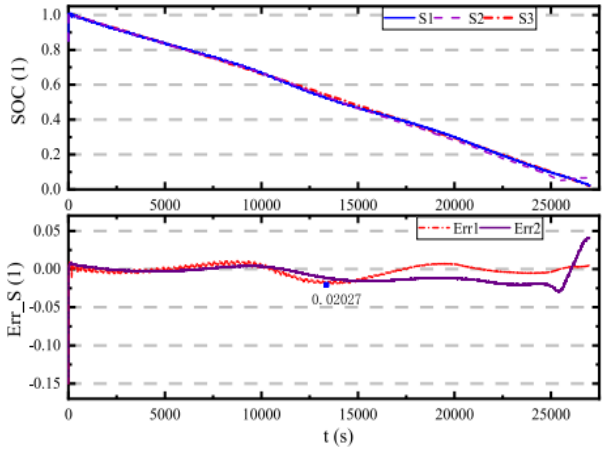

FIGURE 11 SOC estimation under BBDST condition. BBDST, Beijing Bus Dynamic Stress Test; SOC, state of charge [Colour figure can be viewed at wileyonlinelibrary.com]

FIGURE 12 Internal resistance estimation under BBDST condition. BBDST, Beijing Bus Dynamic Stress Test [Colour figure can be viewed at wileyonlinelibrary.com]

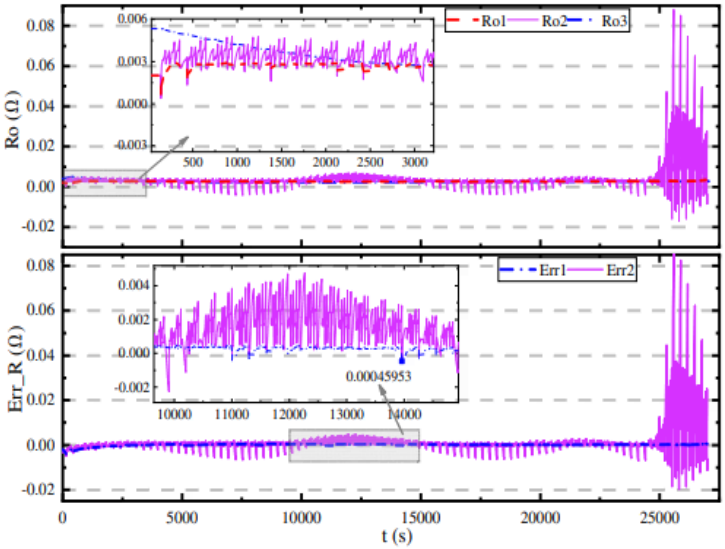

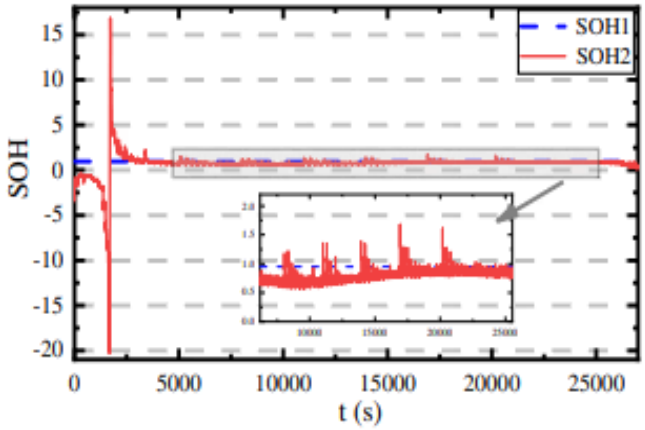

FIGURE 13 SOH estimation under BBDST condition. BBDST, Beijing Bus Dynamic Stress Test; SOC, state of charge [Colour figure can be viewed at wileyonlinelibrary.com]

Tables

TABLE 1 BBDST condition

P_b/kW	P_c/W	t/s	T/s	Status
37.5	37.5	21	21	Starting
72.5	72.5	12	33	Acceleration
4.5	4.5	16	49	Sliding
−15	−15	6	55	Braking
37.5	37.5	21	76	Acceleration
4.5	4.5	16	92	Sliding
−15	−15	6	98	Braking
72.5	72.5	9	107	Acceleration
92.5	92.5	6	113	Rapid acceleration
37.5	37.5	21	134	Acceleration
4.5	4.5	16	150	Sliding
−15	-15	6	156	Braking
72.5	72.5	9	165	Acceleration
92.5	92.5	6	171	Rapid acceleration
37.5	37.5	21	192	Acceleration
4.5	4.5	16	208	Sliding
−35	−35	9	217	Braking
−15	−15	6	229	Braking
4.5	4.5	71	300	Stopping